

# Beam Searching for mmWave Networks with sub-6 GHz WiFi and Inertial Sensors Inputs: an experimental study

Maurizio Rea<sup>a,b</sup>, Domenico Giustiniano<sup>b</sup>, Pablo Jiménez Mateo<sup>b,c</sup>, Yago Lizarribar<sup>b,c</sup>, Joerg Widmer<sup>b</sup>

<sup>a</sup>*Fundació I2CAT, Barcelona, Spain*

<sup>b</sup>*IMDEA Networks Institute, Madrid, Spain*

<sup>c</sup>*University Carlos III of Madrid, Madrid, Spain*

---

## Abstract

Beam training in dynamic millimeter-wave (mm-wave) networks with mobile devices is highly challenging as devices must scan a large angular domain to maintain alignment of their directional beams under mobility. In this work, we exploit the trend of multiple chipsets integrated in the same mobile device to study a set of non-mmwave input data that can be leveraged jointly to provide faster beam search and better data rate. We leverage these findings to introduce SLASH, an algorithm that adaptively narrows the sector search space and accelerates link establishment, link maintenance and handover between mm-wave devices. We experimentally evaluate SLASH with commodity hardware, including a 60 GHz testbed, commercial sub-6 GHz WiFi APs and smartphones. SLASH can increase the median data rate by more than 22% for link establishment and 25% for link maintenance with respect to prior work.

---

## 1. Introduction

Fine beam alignment of the highly directional antennas of mm-wave communication systems is necessary to achieve high data rates or even just a sufficient link margin for communication. The need for fast and efficient beam training strategies has stimulated a variety of research studies, both theoretical and experimental [1–10]. There has been substantial progress in terms of beam training efficiency compared to the original brute force or (optionally) hierarchical training of IEEE 802.11ad. For instance, the compressive beam training approaches only need to scan a subspace of the available antenna beams [11, 9]. Nevertheless, dense deployments with many devices or networks with high mobility remain a challenge. In dense networks with small cell sizes, handovers occur frequently, and a device may need to beam train with potentially many Access Points (APs) to determine to which APs it has the best link quality. In this case, it has been shown that using contextual information can help provide beam steering information to speed up the link establishment without the need for explicit beam training [12, 10].

However, prior works have mainly considered in isolation non mm-wave inputs. Motivated by the availability of multiple chipsets in the same mobile device, we investigate how to jointly use contextual input data, in particular the orientation of the mobile device and its distance and angle to the AP as measured with sub-6GHz legacy WiFi, for speeding up the beam search at mm-wave frequencies. With these inputs, the problems that we aim to address are how to i) maintain beam alignment under device rotation over a very short period of time, ii) reduce beam training delay

exploiting angle information with sub-6 GHz legacy WiFi and channel properties at mmwave frequency, and iii) increase the data rate during the handover process to other APs in range using knowledge of the estimated distance with time measurements extracted with sub-6, GHz legacy WiFi.

We design SLASH, a beam search strategy that exploits out-of-mmwave band contextual input easily available in today's devices. Our contributions are as follows:

- For link establishment, we use angle of arrival extracted from channel state information in sub-6 GHz legacy WiFi as input to narrow down the sector search space. We further exploit the relationship between the quasi-reciprocity of the mm-wave channel to further speed up the link establishment;
- For link maintenance, we propose a fast strategy to maintain the mm-wave link by tracking the device orientation under user mobility through inertial measurements of the mobile device;
- For handover, we use the distance measured with Fine Time Measurements (FTM) integrated in sub-6 GHz legacy WiFi to proactively select the AP to connect to;
- We conduct our studies with experiments with a 60 GHz testbed to validate our approach, and we compare SLASH both to the IEEE 802.11ad standard and prior work. Our study indicates that SLASH is very effective in increasing the data rate with respect to prior work.

## 2. Motivation

mm-wave communication supports physical data rates of several Gb/s using highly-directional phased antenna arrays [13]. Examples of technology using mm-wave are the IEEE 802.11ad standard for Wireless Local Area Networks (WLANs) in the 60 GHz band [14] and 5G cellular networks for licensed mm-wave bands [15]. The communication between AP and User Equipment (UE) in mm-wave requires:

*Link Establishment:* beam training is needed to find the Angle of Departure (AoD) at the transmitter and the Angle of Arrival (AoA) at the receiver in order to select an antenna sector pair that allows to establish communication and maximizes the received power.<sup>1</sup>

*Link Maintenance:* after beam training, environment variations and UE mobility and rotation can cause swift changes of the link quality, and continuous beam adaptation is needed to maintain a high data rate.

*AP handover:* mm-wave network deployments are dense, and multiple APs are presented in the area. Handover procedure must be triggered if there exists an AP that could provide a higher data rate.

### 2.1. Beam training

Beam training is a very time-consuming procedure that leads to high overhead and latency, which in turn wastes network resources and deteriorates the system performance. In this subsection we describe the process for the IEEE 802.11ad beam training.<sup>2</sup> The IEEE 802.11ad standard

---

<sup>1</sup>Note that we interchangeably use the terms sector, beam and pattern.

<sup>2</sup>mm-wave in 5G is under standardization, with beamforming operations for both data and control planes [15, 16].

uses Sector Level Sweep (SLS) to find the optimal AP-UE sector pair based on the highest Signal to Noise Ratio (SNR). SLS consists of two phases: (i) AP SLS and (ii) UE SLS. During the first phase, the AP sends training frames over each of its sectors. This is an exhaustive search that ideally covers the entire  $360^\circ$  azimuth. At the same time, the UE uses a quasi-omnidirectional antenna pattern to receive those training frames, and it identifies the AP sector with the highest SNR. The roles of AP and UE are then switched and the process is repeated again. At the end of this procedure, both devices, AP and UE, know the sectors that maximize the SNR of the link for the communication. Once the link is established, this process will be done again if the link degrades under a certain specific threshold. By doing so, the new combination of sector improves the link quality. According to the standard, the beam refinement phase searches around the current sector pair in order to determine a new combination of beams with improved link quality.

## 2.2. Out-of-mmwave band inputs for beam training

In order to reduce the beam training delay, we investigate how well the AoD/AoA pair providing the highest SNR can be estimated by means of sub-6 GHz WiFi technology, when mm-wave and sub-6 GHz WiFi coexist in the same multi-band device.<sup>3</sup> Previous approaches in this area are affected by three main problems.

**Errors in the angular estimation.** In case of mobile devices, energy and form factor constraints limit the number of antennas to one or two in mobile chipsets [18]. Although APs of typical form factors may have a few antennas, the single antenna used by mobile devices for transmission of 802.11 frames limits the median error in the angle estimation at the AP side to about 20 degrees [19, 20], i.e., even in this case significant further refinement is necessary to ultimately align the antenna beams. This motivates trying alternative approaches that are less demanding in terms of hardware requirements. For this, Channel State Information (CSI) provided by legacy sub-6 GHz technology to infer the direction of the target device must be combined with information of the channel properties at mm-wave to refine the angle estimation for mm-wave communication.

**Inferring angular rotation.** The client rotation must be compensated for any variation of the angle with respect to the spatial reference system and the chosen antenna sector must be adjusted accordingly, otherwise the mm-wave link quality would suffer dramatically. For this purpose, we use contextual information provided by additional inertial sensors embedded in the smartphone, such as the gyroscope.

**Handover procedure at mm-wave.** The client may be connected to the AP until the connection is below the sensitivity before triggering a new search for APs in range. This can cause outage in the communication. We propose to exploit legacy sub-6 GHz technology that can provide distance estimates. For this purpose, we use Fine Time Measurement (FTM) and we provide more details in Sec. 4.2.4.

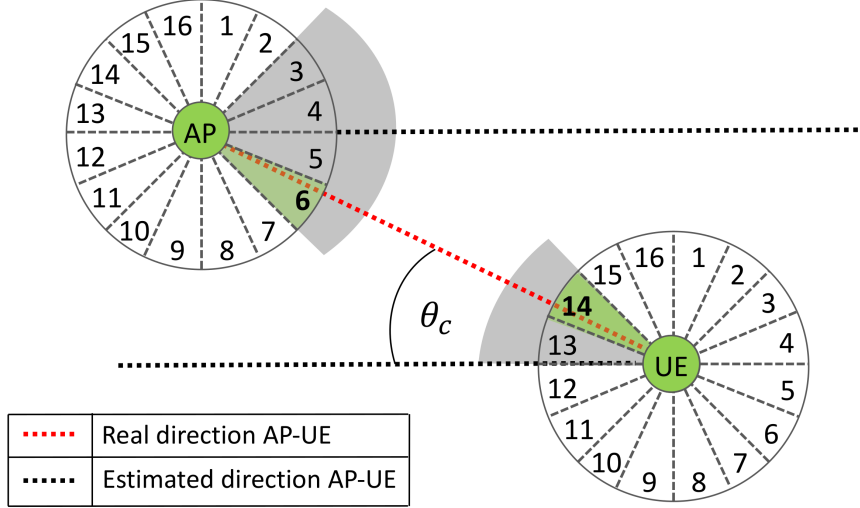
## 3. SLASH with ideal directional antennas

In this section, we present the ideal working principle of SLASH for mm-wave link establishment and maintenance. SLASH is a beam search strategy which exploits input from inertial sensors, channel properties at mm-wave and sub-6 GHz angular information obtained from CSI and ranging estimations from FTM measurements.

---

<sup>3</sup>The sub-6 GHz WiFi radio can also serve as a fallback in case no mm-wave link can be established [17, 15].

### Phase 1: Location-aware AP SLS



### Phase 2: Location-aware UE SLS

Figure 1: Schematic representation of the ideal working principle for link establishment.

#### 3.1. Link establishment

In order to adaptively narrow the sector beam search, we introduce an algorithm for the link establishment. Assuming that AP and UE employ directional antennas for the communication at mm-wave frequencies, we start introducing the AP SLS. At this stage, the AP first exploits the system to retrieve the UE's estimated direction  $\hat{A} \hat{D} A$  and then, fixing the location angle error  $\theta$ , it defines the angular portion  $\Theta^{AP} = 2\theta$ , centered around the line of the UE's estimated direction. Doing so, the AP determines the subset of sectors to probe during the AP SLS.

Fig. 1 shows an example of the proposed link establishment. During the phase 1, the AP transmits training sequences to probe from beams 3 to 6, while the UE receives omnidirectionally and performs SNR measurements.

**Quasi-reciprocity and position of the UE.** For the UE SLS phase, we introduce the concept of channel quasi-reciprocity. The latter, together with the concept of the similarity of the down-link and uplink channels, is usually used for channel estimation [21]. We exploit it in a different way: for the UE SLS phase, we probe the sectors in the direction of the AP,  $\hat{A} \hat{D} D$ , but given that the AP SLS already resolved the angle error at the AP side, we can take this into account to further reduce the number of sectors in the uplink to probe. For the implementation, we set  $\Theta^{UE} = \frac{\Theta^{AP}}{2} = \theta$  for the UE SLS phase. For instance, considering the example in Fig. 1, the correcting effect of AP SLS allows to exclude sectors 11 and 12 from the UE SLS, leaving just two beams (13 and 14) to be probed instead of four. At the end of the two phases, the AP-UE sector pair providing the highest SNR (beams 6 and 14 in the example) is used for data transmission.

Algorithm 1 outlines the pseudo-code of SLASH-LE. Concretely, during the AP SLS phase, the UE is in omnidirectional reception mode, while the AP switches through the  $I$  transmit sectors  $B_i^{AP}$ ,  $i = 1, 2, \dots, I$ , falling within the angular portion  $\Theta^{AP} = 2\theta$ , which can be denoted by the set

$$\mathcal{B}_{AP} = \{B_i^{AP} \text{ falling in } \Theta^{AP}, i = 1, 2, \dots, I\}. \quad (1)$$

---

**Algorithm 1** SLASH-LE

---

**Input:**  $\theta, I, J$ **Phase I:** Direction-aware AP SLS

- 1: UE in omnidirectional reception mode
- 2: Estimate AoA from CSI:  $\hat{A}oA$
- 3:  $\Theta^{AP} = [A\hat{o}A - \theta, A\hat{o}A + \theta]$
- 4: Define  $\mathbf{SNR}_{UE}$  vector
- 5:  $\mathcal{B}_{AP} = \{B_i^{AP} \text{ falling within } \Theta^{AP}, i = 1, 2, \dots, I\}$
- 6: **for**  $i = 1 : I$  **do**
- 7:     AP sends a beacon through sector  $B_i^{AP} \in \mathcal{B}_{AP}$
- 8:     UE stores the measured SNR as  $\mathbf{SNR}_{UE}[i]$
- 9: **end for**
- 10:  $B_{best}^{AP} = B_i^{AP} \in \mathcal{B}_{AP} \text{ --- } \mathbf{SNR}_{UE}[i] = \max(\mathbf{SNR}_{UE})$
- 11: **return**  $B_{best}^{AP}$

**Phase II:** Direction-aware UE SLS

- 12: AP in omnidirectional reception mode
  - 13: Estimate AoD from CSI:  $\hat{A}oD$
  - 14: Compute  $\theta_c$
  - 15:  $\Theta^{UE} = [A\hat{o}D - \theta_c - \theta/2, A\hat{o}D - \theta_c + \theta/2]$
  - 16: Define  $\mathbf{SNR}_{AP}$  vector
  - 17:  $\mathcal{B}_{UE} = \{B_j^{UE} \text{ falling within } \Theta^{UE}, j = 1, 2, \dots, J\}$
  - 18: **for**  $j = 1 : J$  **do**
  - 19:     UE sends a beacon through sector  $B_j^{UE} \in \mathcal{B}_{UE}$
  - 20:     AP stores the measured SNR as  $\mathbf{SNR}_{AP}[j]$
  - 21: **end for**
  - 22:  $B_{best}^{UE} = B_j^{UE} \in \mathcal{B}_{UE} \text{ --- } \mathbf{SNR}_{AP}[j] = \max(\mathbf{SNR}_{AP})$
  - 23: **return**  $B_{best}^{UE}$
- 

The UE performs SNR omnidirectional measurements over the set of beams trained by the AP and selects the  $B_{best}^{AP}$  as the beam providing maximum SNR. In the subsequent UE SLS phase, the UE uses the estimated direction of the AP and corrects it by the angle  $\theta_c$  inferred from the AP SLS results. Training packets are transmitted by the UE switching across the  $J$  sectors  $B_j^{UE}$ ,  $j = 1, 2, \dots, J$ , falling within the angular portion  $\Theta^{UE} = \theta$ , which can be denoted by the set

$$\mathcal{B}_{UE} = \{B_j^{UE} \text{ falling in } \Theta^{UE}, j = 1, 2, \dots, J\}. \quad (2)$$

As before, the AP performs SNR omnidirectional measurements over the set of UE transmit sectors and selects  $B_{best}^{UE}$  as the beam providing maximum SNR. At the end of the procedure, AP and UE enter the data transmission phase where the selected beams  $B_{best}^{AP}$  and  $B_{best}^{UE}$ , respectively, are used to communicate.

### 3.2. Link maintenance

We propose an algorithm to maintain the mm-wave communication and update the current sector using data from the gyroscope and the compass of the smartphone for rotation estimation. Furthermore, SLASH uses data from FTM measurements to monitor the distances between the UE and all the available APs.

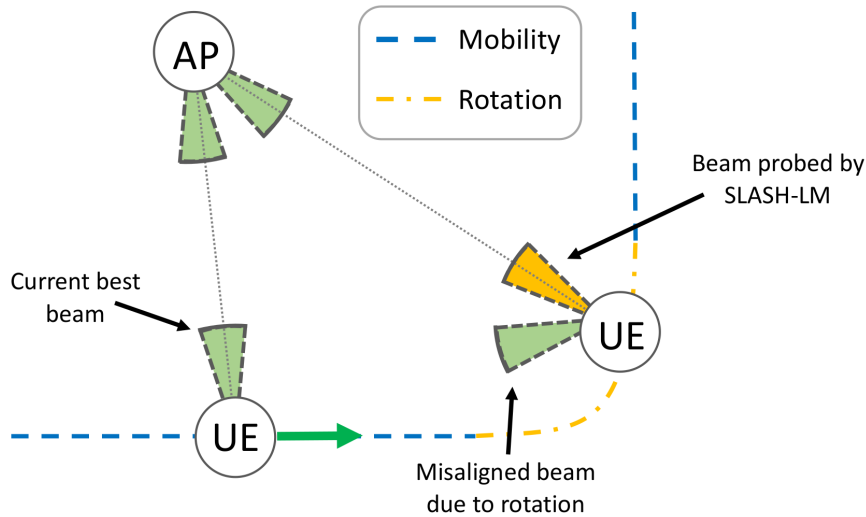


Figure 2: Illustrative example of link maintenance using SLASH.

As we consider static APs, UE rotations imply that only the antenna sector at the UE side needs to be updated. The key is that, while the optimal beam for the AP may not change a lot (especially if the mobile device is not very close to the AP), this is not the case with the mobile device, where each rotation can significantly impact the optimal beam.

The main algorithm steps are as follows:

- During UE mobility, as soon as the system observes a drop in signal quality, the estimated angular rotation since the last link maintenance is determined.
- If the angular velocity indicates a change in direction, the two candidate sectors are trained following a UE SLS-like approach.
  - The new direction with the highest SNR is selected for mm-wave communication. Any error in the estimated angular velocity is immediately solved using the direction with the highest mm-wave SNR as feedback loop.
- If the angular velocity indicates no changes in direction and the mm-wave link quality is low, SLASH monitors the distance estimates from the UE to the AP.
  - Beam refinement/tracking as defined by the 802.11ad standard is used when the distance estimate indicates that the UE is connected to the closest AP (cf. Section 2.1). We emphasize that this procedure is different from the full SLS.
  - A handover procedure is instead triggered when the distance estimates indicate that there is a closer AP.

#### 4. Deployment and Experimental Platforms

In this section we first introduce the deployment scenario and then the experimental platforms for the evaluation of SLASH during link establishment and link maintenance.

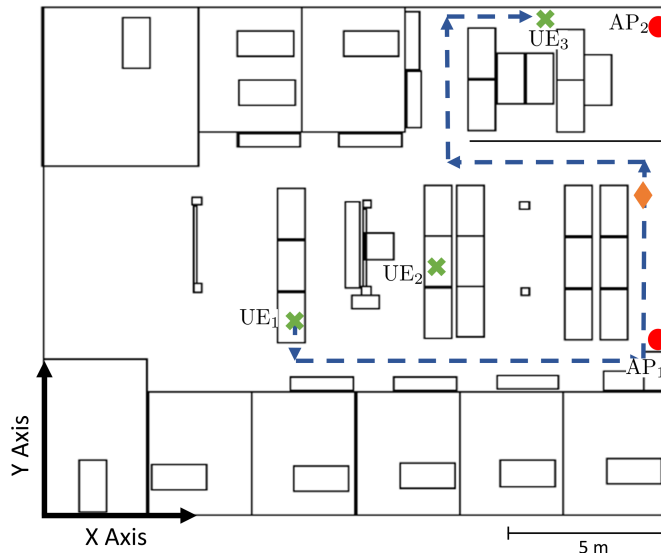


Figure 3: Indoor environment considered for static and mobile tests.

#### 4.1. Scenario

Our measurements are conducted in an indoor space with an open area and offices covering a total area of  $300 \text{ m}^2$ . This testbed contains several obstructions, and concrete walls and glasses separate the offices from the open area. The map of the scenario is shown in Fig. 3, where green crosses mark three random selected UE positions and red circles mark the AP positions that have a distance of 9.7 meters between them. For the evaluation of SLASH, each AP is equipped with 60 GHz transceiver in order to perform mm-wave measurements. In the same positions, after collecting data at 60 GHz, we also deploy the sub-6 GHz devices to infer context information.

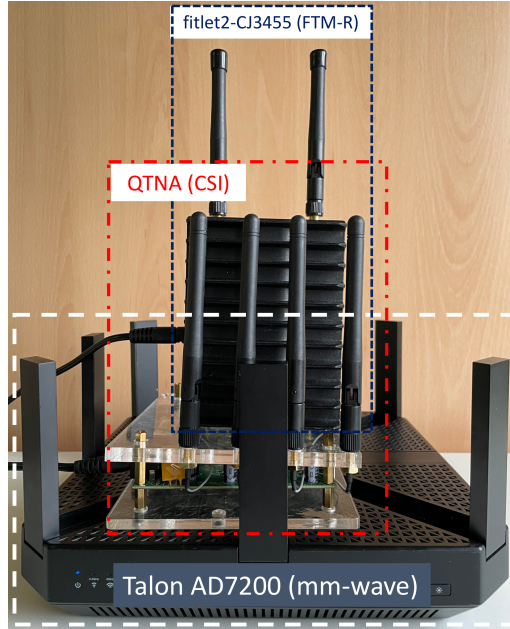
#### 4.2. Experimental Platforms

In this Section we describe how to combine all the components needed for running the proposed solution for speeding up the beam search at mm-wave frequencies. An illustration of the commodity hardware we use for the AP is shown in Fig. 4(a). While being associated to the WiFi chipset performing AOA measurements, the STA sends FTM requests to the FTMR (using a different WiFi chipset). This is possible since the FTM protocol allows the initiator to exchange FTM packets without the need to be associated to the WiFi AP. Doing so, the AP can collect both AOA and distance measurements.

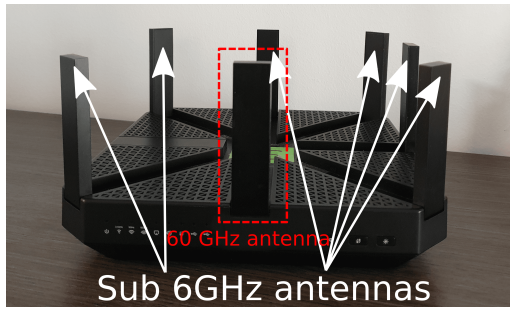
While collecting these measurements, the AP is connected at 60 GHz to the UE, and, as explained in Section 2.2, it uses the information collected from inertial sensors and at sub-6 GHz for communication in the mmWave band. We post-process the results using MATLAB. In the next subsections we provide details about the single components.

##### 4.2.1. 60 GHz

In order to perform measurements at 60 GHz, we use as AP a Talon AD7200 device, shown in Fig. 4(b). The AP consists of 5 sub-6 GHz antennas and a single 60 GHz antenna array with 32 antenna elements and it supports IEEE 802.11ad protocol. Thanks to a firmware modification,



(a) Experimental setup used for measurements.



(b) Setup for measurements at 60 GHz for SLASH-LE and



(c) Setup for sub-6 GHz CSI measurements during SLASH-LE procedure.

Figure 4: Experimental platforms used for running the proposed solution for speeding up the beam search at mm-wave frequencies.

Talon AD7200 enables rapid collection of SNR during SLS phases, as seen in [22]. The SNR measurements extracted by the firmware are quantized in quarters of dB in a range from -7 to 12 dB. However, due to manufacturing constrains and cost reduction decisions, the measured beam patterns are not ideal and they do not present a main lobe in a specific direction. Fig. 5 illustrates some measured beam patterns, out of 35 predefined patterns (34 Tx patterns plus one quasi-omnidirectional Rx pattern), of the Talon AD7200's antenna array.

#### 4.2.2. CSI from sub-6 GHz

In order to collect CSI measurements, we use the Quantenna (QTNA) device, shown Fig. 4(c). More specifically, QTNA presents 4 antennas in a Uniform Linear Array (ULA) and it supports 802.11 a/n/ac protocol. The bandwidth can be set between 20, 40 and 80 MHz and the frequency range is from 5.15 GHz to 5.85 GHz. The fact that the QTNA presents 4 antennas in a ULA causes ambiguity problem in case the UE are on right side of the AP positions, referring to the map shown in Fig. 3. For this reason, we consider a deployment of the APs for which this kind of ambiguity cannot be detected. Depending on the scenario under study, a possible solution could be the deployment of the antennas in a non linear array, such as for instance rectangular and circular.

In order to collect MIMO CSI data, we connect the QTNA to an Host PC via ethernet. Doing so, once the UE is connected to the QTNA device, we are able to capture binary data of 4x1 channels with 80 MHz of bandwidth, over TCP on the Host PC. We then convert the obtained binary file to another format for an offline analysis in MATLAB. At the UE side, any WiFi device can be used. The extracted channel is a  $N \times M$  complex matrix, where  $N$  is the number of subcarriers and  $M$  the number of antennas. In order to identify the strongest angle (AoA and AoD), we use the MUltiple SIgnal Classification (MUSIC) algorithm [23]. The latter is a very well known technique based on the subspace decomposition of the covariance matrix.

#### 4.2.3. Inertial Sensors

With the purpose of collecting gyroscope and compass data, we develop an Android application to retrieve the values from the gyroscope sensor. We use the Google Pixel 3 for our experiments. The data are collected throughout the path, with a sampling rate of 50 samples per second. Gyroscope data are obtained through the calibrated sensor events readily available in the Android SDK, which compensate for the observed drift in the inertial measurements along all the axes of the device. All data are then passed through a simple low pass filter to remove the higher frequency noise in the measurements. The whole analysis assumes that the UE has a fixed relative orientation (e.g. placed always vertically). In more complex cases it is needed the relative orientation of the UE, which could be provided by the gyroscope.

When performing the experiment, the device is held at an angle of  $90^\circ$  with respect to the ground so that the rotation is predominantly visible on the vertical axis of the mobile device and speed is kept constant except for the turning points in the pathway. Gyroscope is preferred over the magnetometer of the smartphone, as it is not affected by metallic objects in the environment and provides sufficient information for assisting the beam procedure.

#### 4.2.4. Configuration for handover

For triggering the handover procedure, we use FTM measurements from legacy WiFi. According to the FTM protocol standardized by IEEE 802.11-2016, a single FTM measurement is an estimation of the distance between a pair of WiFi devices, called responder (FTM-R) and initiator (FTM-I). More specifically, the latter is a UE that starts the FTM process by sending a first request to the FTM-R that is the corresponding AP. Then, once the FTM-R agrees on performing the measurements, it sends a FTM message, waiting until its ACK. Storing the timestamp at the transmission of the FTM message and the one at the reception of the ACK, and knowing the propagation speed in the air, the estimated distance is calculated.

For this purpose, we use a filetel2-CJ3455 device with the WiFi Intel 8265 chipset as FTM-R, and a Google Pixel 3 phone with Android Pie as FTM-I device. Furthermore, we use an Android

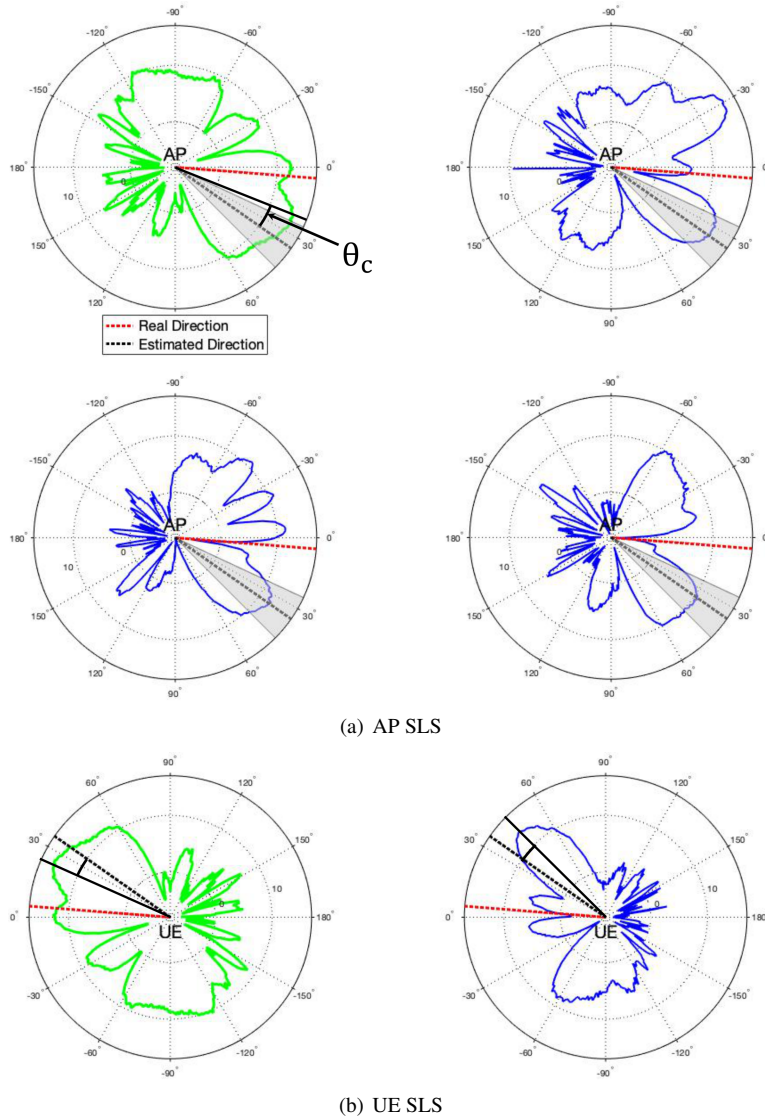


Figure 5: Representation of the real working principle for link establishment, using Talon AD7200 beam patterns. We select the first 4 and 2 candidate patterns for AP SLS and UE SLS, respectively.

application to initiate the measurements and to facilitate the data collection. Having the list of all available APs, we then select the FTM-R in order to display and store the estimated distance between the latter and the smartphone.

We note that, as our system is a prototype that requires different hardware to run each WiFi chipset, the distance between these chipsets is in the order of ten cm, much larger than with an integrated chipset with multiple transceivers.

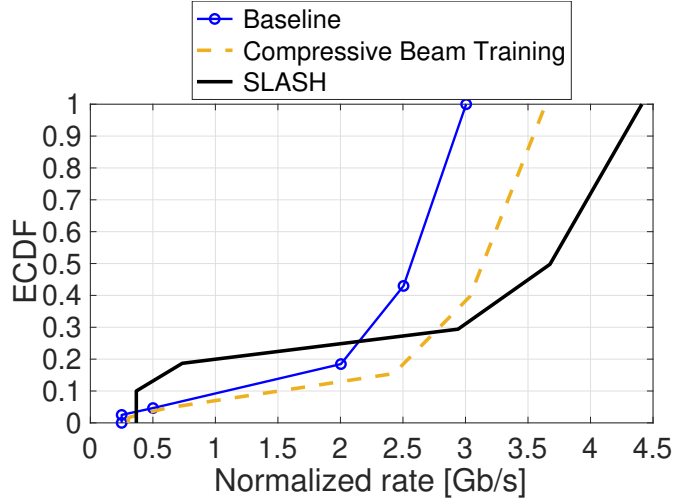


Figure 6: ECDF of the normalized mm-wave data rate for different beam search strategies.

## 5. System evaluation

In this section, we first introduce the real working principle of SLASH, using real beam patterns extracted from the hardware described in Sec. 4.2.1. We then evaluate the performance of our proposed algorithm in static and mobile scenarios, comparing it against existing solutions in the literature.

### 5.1. From ideal to measured beam patterns

In this subsection we describe how to adapt the ideal working principle of SLASH, presented in Sec. 3, using the real Talon AD7200 beam patterns, introduced in Sec. 4.2.1. Fig. 5 shows a real example of SLS procedure for a specific link establishment ( $AP_1$  and  $UE_1$  in Fig. 3). Starting with AP SLS as first stage, the AP retrieves the UE's estimated direction  $\hat{A}\hat{o}A$  through CSI measurements. Knowing the angular portion  $\Theta^{AP}$ , we sort the 34 Tx available patterns according to the power radiated within the selected region, centered around the line of  $\hat{A}\hat{o}A$ . The key is that, higher is this value, higher is the probability to select this beam. The UE performs SNR omnidirectional measurements over the set of the first 4 sorted beams trained by the AP, and it selects  $B_{best}^{AP}$ . We then calculate the angle error  $\theta_c$  as the angle between the UE's estimated direction and the direction of the maximum SNR detected in  $B_{best}^{AP}$  (green beam pattern in Fig. 5(a)). Thanks to the channel reciprocity principle introduced in Figure 1, in the subsequent UE SLS phase, the UE corrects the  $\hat{A}\hat{o}D$  by the angle  $\theta_c$  and it selects as possible candidates the 2 beam patterns (instead of 4) where their directions of the maximum SNR are  $\hat{A}\hat{o}D-\theta_c$  and  $\hat{A}\hat{o}D+\theta_c$ . As before, the AP performs SNR omnidirectional measurements over the set of UE transmit sectors and it selects  $B_{best}^{UE}$  (green beam pattern in Fig. 5(b)).

### 5.2. SLASH-LE for a static user

We consider a user in three static positions ( $UE_1$ ,  $UE_2$  and  $UE_3$  in Fig. 3) that performs the link establishment phase for all two APs, through the SLASH algorithm presented in Sec. 3.1. We evaluate the ability of SLASH to accelerate the link establishment between AP and UE. We

compute the normalized data rate as  $R \cdot \frac{T}{T+\tau}$ , where  $R$  is the achieved data rate,  $T = 2$  ms is the data frame size, and  $\tau$  is the beam search latency.

As a result of the successful beam search completion, the final data rate  $R$  over the directional 60 GHz link established between AP and UE can be computed for the configured beams  $B_{best}^{AP}$  and  $B_{best}^{UE}$ . More specifically, the *experimental SNR* values in a 2-GHz bandwidth at 60 GHz can be translated into an achievable bit-rate  $R$  following an IEEE 802.11ad specific rate table [14].

In order to measure the beam search latency, we consider the typical duration of training packets according to the 802.11ad standard (15.8  $\mu$ s). In Fig. 6 we compare SLASH with other two different strategies, the IEEE 802.11ad as "Baseline" and [9] ("Compressive Beam Training"). "Compressive Beam Training" adapts compressive path tracking for sector selection. The ECDFs show that SLASH achieves a data rate that is 22% higher in median than "Compressive Beam Training". Performance loss at lower percentiles are caused by the errors in the experimental angle estimation at sub-6 GHz with MUSIC algorithm. In practical cases, SLASH can achieve even higher performance than prior work, as it can exploit the estimated direction of the UE.

### 5.3. SLASH for a mobile user

We study the performance of SLASH with a user moving along the mobility pattern in Fig. 3, which includes straight-line paths and rotations.

For the experimental trace, the mobile user holds the UE, walks along the trajectory at an approximated speed of 0.5 m/s and rotates at an approximated rotation speed of 0.35 rad/s. In the map in Fig. 3, we show the real trajectory of the user with the blue dashed line and we use an orange diamond for the position where the user performs a handover to the second AP. For the study, we use as input real distance estimates using FTM measurements from each of the APs (see Section 4.2.4). In real systems, the sub-6 GHz chipset is in close proximity to the mm-wave chipset, and therefore FTM estimates can be used to estimate the distance between the mm-wave antennas at the transmitter and receiver. The trace used for the evaluation of FTM accuracy is shown in the first plot of Fig. 7. As it can be seen in the figure, the distance between the UE and the  $AP_1$  (yellow line) and  $AP_2$  (green line) is estimated with a median error of 1.8 and 4.1 meters, respectively.

We evaluate the normalized data rate along the whole trajectory for four different algorithms. The results are shown in Fig. 7, where "Constant Error Method" indicates the strategy in [24]. For the study, we use as input real distance estimates using FTM measurements from each of the APs. The trace used for the evaluation is shown in the central plot in Fig. 7. SLASH tries to maintain the highest data rate, and the algorithm is called as soon as the SNR drops below the threshold for communication at the highest data rate. In addition, the user performs the handover to  $AP_2$  using distance measurement inputs. Other strategies performs a handover only when the mm-wave link is below the threshold for communication. However, this does not occur in the open space under study. The plot shows the time when the link maintenance is triggered due to the rotation. The "Baseline", "Constant Error Method" and "Compressive Beam Training" approaches are not able to detect rotation events and, therefore, need to resort to the same full beam search used for link establishment. Along the whole trajectory, SLASH achieves a median data rate 25% higher than "Compressive Beam Training" and 34% higher than other strategies.

## 6. Related work

The problem of fast mm-wave link establishment and maintenance is widely discussed in the literature. A comparative analysis of initial access techniques in mm-wave networks is presented

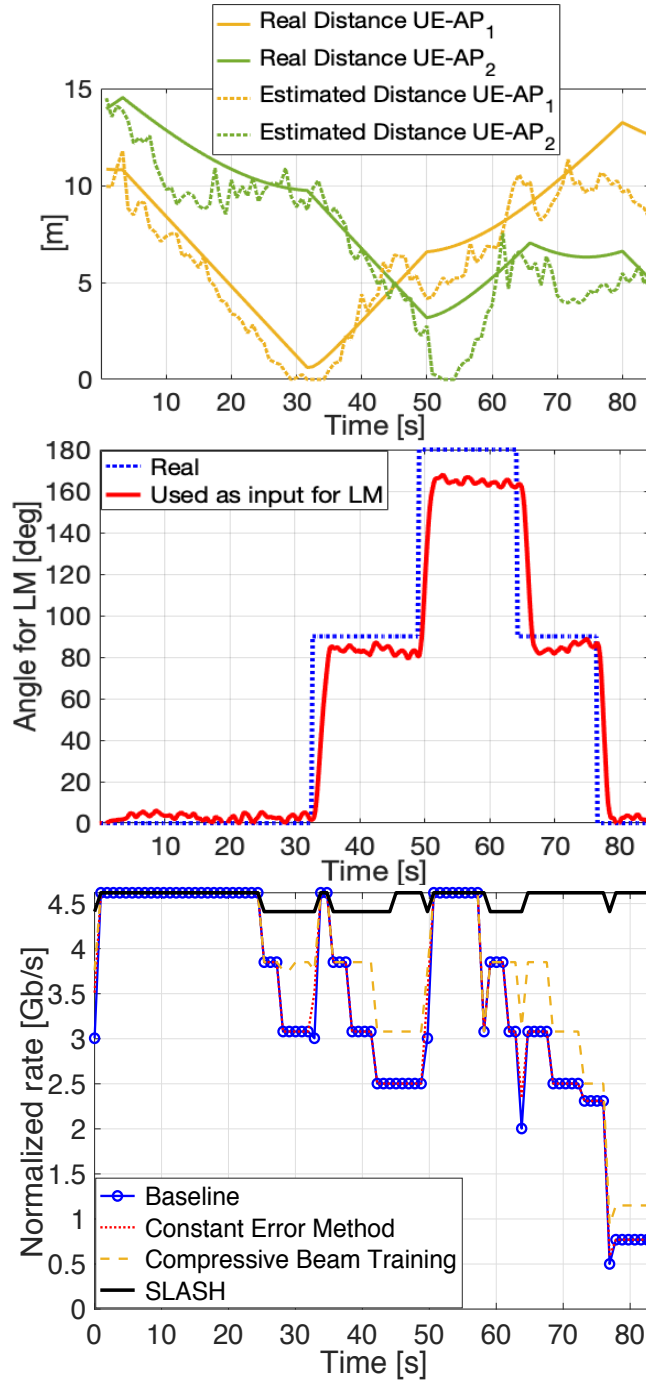


Figure 7: Context-aware information, and data rate of SLASH and other algorithms.

in [1]. Simultaneous transmissions from multiple direction-coded beams to accelerate the beam search are exploited in [2, 3]. In [25] the authors use multi-lobe antenna patterns with random phase shifts for the beam training, which enables compressive sensing approaches to determine AoA and AoD. This approach requires arbitrary phase shifters over the antenna elements, which is not supported by standard off-the-shelf mm-wave devices that operate with low-resolution (2-bit) RF phase shifters [26].

In [4], a link-level measurement study of indoor 60 GHz networks using a software-radio platform revealed several challenges related to human blockage and device motion and how they affect the design of MAC protocols. Some of the findings of that work have been applied to extract context information from mm-wave networks in BeamSpy [27]. BeamSpy presents a beam tracking prediction mechanism based on the channel sparsity and spatial correlation of the 60 GHz link. The proposed approach works only in static conditions, while we target mobile users. Mm-wave and sub-6 GHz WiFi context information can complement each other and can enrich the set of inputs provided for the design of MAC protocols. [9] uses compressive sensing to sweep only through a subset of probing sectors.

Only very few works in the literature address the problem of fast beam search in realistic, dynamic scenarios with node mobility. In [5], a protocol for mobility resilience and overhead constrained adaptation for directional 60 GHz links is presented. A “beam sounding” mechanism is introduced to estimate the link quality for selected beams, and identify and adapt to link impairments. In [28] the authors develop a zero overhead beam tracking mechanism that uses two different beam patterns during the preamble of the frames. This allows to estimate user rotation and movement. The approach does not use context information from out-of-band channels, and it requires changes in the preamble structure. In [10] an algorithm that removes in-band overhead for directional mm-wave link establishment is proposed. However, the study focuses only on static scenarios without rotation, and requires at least five antennas in both the sub-6 GHz transmitter and receiver to achieve a similar angle error as in our system.

[6] relies on gyroscope sensors only to reduce the beam search under mobility, while we also use other context information available in sub-6 GHz WiFi. More specifically, they utilize the previously valid link knowledge to initialize a new beam search, and adaptively extend the search range to determine the new link. The coupling of legacy technology together with mm-wave frequencies in order to improve the beam search has been studied in some recent work. In [29], it is shown that beam training and cell discovery, respectively, can be accelerated assuming the availability of Global Positioning System (GPS) information about device locations.

In [30] we already introduced SLASH algorithm, showing through extensive simulations and experiments its capability to significantly increase the data rate compared to prior work. More specifically, [30] computed the ToF distance estimate using 802.11 data/ACK handshake. It fixed the AoA estimation based on the median angle error presented in [10], and it assumed that rotation information is subjected to an error of a few degrees. For tests in mobility, [30] adopted the well known ray-tracing based signal propagation tool WinProp. On the contrary, this work uses the new FTM protocol for the estimation of the distance and it investigates CSI data at sub-6 GHz for AoA estimation. We also collect data from inertial sensors of a smartphone for inferring angular rotation and we perform measurements at 60 GHz for SLASH evaluation in static and mobile scenarios.

## 7. Conclusion

In this work we investigated how context information from various out-of-band inputs such as channel state information and fine time measurements from legacy WiFi devices as well as from the inertial sensors of the smartphone can be used jointly to speed-up the beam training process in mm-wave networks. We have then introduced SLASH, an algorithm to perform beam search for link establishment and maintenance. We have shown through extensive experiments that SLASH can significantly increase the data rate of mobile users compared to prior work. Our mechanism has the potential to be integrated in multi-band WiFi devices.

## Acknowledgment

This research work was sponsored in part by the European Union's Horizon 2020 research and innovation programme under Grant No. 871249 (LOCUS), and in part by Ministerio de Ciencia, Innovación y Universidades (MICIU) grant RTI2018-094313-B-I00 (PinPoint5G+).

## References

- [1] M. Giordani, M. Mezzavilla, C. N. Barati, S. Rangan, and M. Zorzi, "Comparative analysis of initial access techniques in 5G mmWave cellular networks," in *2016 Annual Conference on Information Science and Systems (CISS)*, March 2016.
- [2] Y. Tsang, A. Poon, and S. Addepalli, "Coding the beams: Improving beamforming training in mmwave communication system," in *2011 IEEE Global Telecommunications Conference (GLOBECOM)*, Houston, TX, USA, Dec. 2011.
- [3] L. Chen, Y. Yang, X. Chen, and W. Wang, "Multi-stage beamforming codebook for 60GHz WPAN," in *2011 6th Int. ICST Conference on Communications and Networking in China (CHINACOM)*, Aug. 2011.
- [4] S. Sur, V. Venkateswaran, X. Zhang, and P. Ramanathan, "60 ghz indoor networking through flexible beams: A link-level profiling," in *ACM SIGMETRICS Performance Evaluation Review*, vol. 43, no. 1, 2015, pp. 71–84.
- [5] M. K. Haider and E. W. Knightly, "Mobility resilience and overhead constrained adaptation in directional 60 ghz wlans: protocol design and system implementation," in *Proceedings of the 17th ACM International Symposium on Mobile Ad Hoc Networking and Computing*. ACM, 2016, pp. 61–70.
- [6] A. Patra, L. Simić, and M. Petrova, "Experimental evaluation of a novel fast beamsteering algorithm for link re-establishment in mm-wave indoor wlans," in *27th Annual IEEE International Symposium on Personal, Indoor and Mobile Radio Communications (PIMRC)*, Sept. 2016.
- [7] A. Alkhateeb, O. E. Ayach, G. Leus, and R. W. Heath, "Channel estimation and hybrid precoding for millimeter wave cellular systems," *IEEE Journal of Selected Topics in Signal Processing*, vol. 8, no. 5, pp. 831–846, Oct. 2014.
- [8] D. De Donno, J. Palacios, D. Giustiniano, and J. Widmer, "Hybrid analog-digital beam training for mmWave systems with low-resolution RF phase shifters," in *2016 IEEE ICC Workshop on 5G RAN Design*, May 2016.
- [9] D. Steinmetzer, D. Wegemer, M. Schulz, J. Widmer, and M. Hollick, "Compressive millimeter-wave sector selection in off-the-shelf IEEE 802.11ad devices," in *Proceedings of the 13th International Conference on Emerging Networking EXperiments and Technologies*, ser. CoNEXT '17. New York, NY, USA: ACM, 2017, pp. 414–425. [Online]. Available: <http://doi.acm.org/10.1145/3143361.3143384>
- [10] T. Nitsche, A. B. Flores, E. W. Knightly, and J. Widmer, "Steering with eyes closed: mm-wave beam steering without in-band measurement," in *2015 IEEE Conference on Computer Communications (INFOCOM)*. IEEE, 2015, pp. 2416–2424.
- [11] M. E. Rasekh, Z. Marzi, Y. Zhu, U. Madhoo, and H. Zheng, "Noncoherent mmwave path tracking," in *Proceedings of the 18th International Workshop on Mobile Computing Systems and Applications*, 2017.
- [12] A. Capone, I. Filippini, and V. Sciancalepore, "Context information for fast cell discovery in mm-wave 5g networks," in *Proceedings of European Wireless 2015*. VDE, 2015, pp. 1–6.
- [13] T. S. Rappaport, R. M. S. Sun, H. Zhao, Y. Azar, K. Wang, G. N. Wong, J. K. Schulz, M. Samimi, and F. Gutierrez, "Millimeter wave mobile communications for 5G cellular: It will work!" *IEEE Access*, vol. 1, pp. 335–349, May 2013.
- [14] IEEE standard, "IEEE 802.11ad WLAN enhancements for very high throughput in the 60 GHz band," 2012.

- [15] 3GPP, “Tr 38.802,” in *Study on New Radio (NR) Access Technology - Physical Layer Aspects - Release 14*, 2017.
- [16] —, “Ts 38.811,” in *NR - Physical Channels and Modulation - Release 15*, 2017.
- [17] S. Sur, I. Pefkianakis, X. Zhang, and K.-H. Kim, “Wifi-assisted 60 ghz networks,” in *ACM International Conference on Mobile Computing and Networking*, ser. ACM Mobicom, 2017.
- [18] —, “Practical MU-MIMO user selection on 802.11ac commodity networks,” in *Proceedings of the 22Nd Annual International Conference on Mobile Computing and Networking*, ser. MobiCom '16. New York, NY, USA: ACM, 2016, pp. 122–134.
- [19] S. Sen, J. Lee, K.-H. Kim, and P. Congdon, “Avoiding multipath to revive inbuilding wifi localization,” in *Proceeding of the 11th Annual International Conference on Mobile Systems, Applications, and Services*, ser. MobiSys '13. New York, NY, USA: ACM, 2013, pp. 249–262. [Online]. Available: <http://doi.acm.org/10.1145/2462456.2464463>
- [20] J. Gjengset, J. Xiong, G. McPhillips, and K. Jamieson, “Phaser: Enabling phased array signal processing on commodity wifi access points,” in *Proceedings of the 20th Annual International Conference on Mobile Computing and Networking*, ser. MobiCom '14. New York, NY, USA: ACM, 2014, pp. 153–164. [Online]. Available: <http://doi.acm.org/10.1145/2639108.2639139>
- [21] Q. Gao, F. Qin, and S. Sun, “Utilization of channel reciprocity in advanced mimo system,” in *2010 5th International ICST Conference on Communications and Networking in China*, Aug 2010, pp. 1–5.
- [22] D. Steinmetzer, D. Wegemer, M. Schulz, J. Widmer, and M. Hollick, “Compressive Millimeter-Wave Sector Selection in Off-the-Shelf IEEE 802.11ad Devices,” in *Proceedings of the 13th International Conference on Emerging Networking EXperiments and Technologies*, ser. CoNEXT '17. New York, NY, USA: Association for Computing Machinery, 2017, p. 414–425. [Online]. Available: <https://doi.org/10.1145/3143361.3143384>
- [23] R. Schmidt, “Multiple emitter location and signal parameter estimation,” *IEEE Transactions on Antennas and Propagation*, vol. 34, no. 3, pp. 276–280, March 1986.
- [24] W. B. Abbas and M. Zorzi, “Context information based initial cell search for millimeter wave 5g cellular networks,” in *2016 European Conference on Networks and Communications (EuCNC)*, June 2016, pp. 111–116.
- [25] O. Abari, H. Hassanieh, M. Rodriguez, and D. Katabi, “Millimeter wave communications: From point-to-point links to agile network connections,” in *Proceedings of the 15th ACM Workshop on Hot Topics in Networks*, 2016.
- [26] A. Alkhateeb, O. E. Ayach, G. Leus, and R. W. Heath, “Channel estimation and hybrid precoding for millimeter wave cellular systems,” *IEEE Journal of Selected Topics in Signal Processing*, vol. 8, no. 5, pp. 831–846, Oct 2014.
- [27] S. Sur, X. Zhang, P. Ramanathan, and R. Chandra, “Beamspy: Enabling robust 60 ghz links under blockage,” in *Proceedings of the 13th Usenix Conference on Networked Systems Design and Implementation*, ser. NSDI'16. Berkeley, CA, USA: USENIX Association, 2016, pp. 193–206. [Online]. Available: <http://dl.acm.org/citation.cfm?id=2930611.2930625>
- [28] A. Loch, H. Assasa, J. Palacios, J. Widmer, H. Suys, and B. Debaillie, “Zero overhead device tracking in 60 ghz wireless networks using multi-lobe beam patterns,” in *Proc. ACM CoNEXT*, 2017.
- [29] W. B. Abbas and M. Zorzi, “Context information based initial cell search for millimeter wave 5G cellular networks,” in *2016 European Conference on Networks and Communications (EuCNC)*, June 2016, pp. 111–116.
- [30] M. Rea, D. Giustiniano, G. Bielsa, D. De Donno, and J. Widmer, “Beam search strategy for millimeterwave networks with out-of-band input data,” in *2020 Mediterranean Communication and Computer Networking Conference (MedComNet)*, 2020, pp. 1–8.